

Generalized parton distributions of the pion in a Bethe-Salpeter approach

L. Theußl,^{*} S. Noguera,[†] and V. Vento[‡]

*Departamento de Física Teórica and Instituto de Física Corpuscular,
Universidad de Valencia-CSIC, E-46100 Burjassot (Valencia), Spain.*

(Dated: February 9, 2020)

We calculate generalized parton distribution functions in a field theoretic formalism using a covariant Bethe-Salpeter approach for the determination of the bound-state wave function. We describe the procedure in an exact calculation in scalar electrodynamics proving that relevant corrections outside our scheme vanish. We extend the formalism to the Nambu – Jona-Lasinio model, a realistic theory of the pion. We go in both cases beyond all previous calculations and discover that all important features required by general physical considerations, like symmetry properties, sum rules and the polynomiality condition, are explicitly verified. We find that in the Nambu – Jona-Lasinio calculation, the generalized parton distributions do not vanish at the kinematic boundary regions, i.e. at $x = 0$ and $x = 1$, while they do in the scalar model. We discuss the possible origin of the boundary behavior.

PACS numbers: 24.10.Jv, 11.10.St, 13.40.Gp, 13.60.Fz

I. INTRODUCTION

Hard reactions provide important information for unveiling the structure of hadrons. The large virtuality, Q^2 , involved in these processes allows the factorization of the hard (perturbative) and soft (non-perturbative) contributions in their amplitudes. Therefore these reactions are receiving great attention by the hadronic physics community. Among the hard processes, the Deeply Virtual Compton Scattering (DVCS) merits to be singled out, because it can be expressed, in the asymptotic regime, in terms of the so called Generalized Parton Distributions (GPDs) [1, 2, 3, 4]. The GPDs describe non-forward matrix elements of light-cone operators and therefore measure the response of the internal structure of the hadrons to the probes [5, 6, 7, 8]. There is much effort under way related to the measurement of these functions.

Due to the impossibility at present to determine the GPDs from Quantum Chromodynamics directly, models have been used to provide estimates which should serve to guide future experiments [9, 10, 11, 12, 13, 14]. The aim of our work is to perform such a calculation in a field theoretic scheme which treats the bound-state in a fully covariant manner following the Bethe-Salpeter approach. In this way we would like to preserve all invariances of the problem. For simplicity we shall use mesons as initial and final states.

We define a scheme, to calculate the electro-magnetic interaction of hadrons, which separates the soft parts, where we use a non perturbative treatment, and the hard parts, where the conventional perturbative treatment is applied. The scheme preserves gauge invariance to leading order and leading twist.

In order to describe the soft part we start by using as a test of our ideas a model based on the ϕ^4 field theory. This theory has the advantage of being renormalizable and therefore any contribution can be analyzed properly. We show, for example, that a correction to the hand bag contribution to first order in the strong coupling constant, which goes beyond our scheme, vanishes.

We next proceed to the main development of this paper, namely to perform the study of the GPDs of the pion by using the Nambu - Jona Lasinio (NJL) model to describe its structure. The NJL model is not a toy model. In fact, it is the most realistic model for the pion based on a quantum field theory built with quarks. It gives a good description of the low energy physics of the pion and respects the realization of chiral symmetry [15]. Moreover it has been used as the model to tune many coefficients of Chiral Perturbation Theory [16].

The NJL model is a non renormalizable field theory and therefore a cut-off procedure has to be defined. We have chosen the Pauli-Villars regularization procedure because it respects all the symmetries of the problem. In our scheme, we use the NJL model to describe the soft (non perturbative) part of the process, i.e. the initial and final states, while for the hard part we use conventional perturbative QCD. The use of the NJL model allows to calculate the GPDs for

^{*}Electronic address: Lukas.Theussl@uv.es

[†]Electronic address: Santiago.Noguera@uv.es

[‡]Electronic address: Vicente.Vento@uv.es

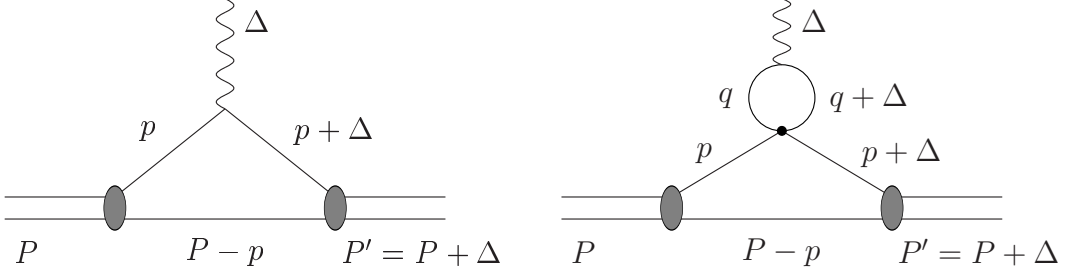


FIG. 1: Overlap diagrams up to order g for the elastic form factor.

massive pions. Some peculiarities, as the non vanishing of the GPDs at the kinematic boundary regions, $x = 0$ and $x = 1$, well known in the exact $m_\pi = 0$ limit, survive when $m_\pi \neq 0$.

Our paper is organized as follows. In section II we give some general definitions for scalar partons and we introduce our kinematical variables. In section III and IV we will define our approach for the scalar and the NJL model respectively. Section V presents our results and Section VI our conclusions.

II. GENERAL FORMULAS AND KINEMATICS

The GPDs are non-diagonal matrix elements of bi-local field operators. Various conventions, reference frames, variables, etc., have been used in the literature for the description of such objects. Our notation is represented in Fig. 1, i.e., the initial momentum is labeled by P , the final momentum by P' , and the momentum transfer is given by $\Delta = P' - P$. We shall describe initially a model with scalar particles, the generalization to particles with spin is straightforward and will be outlined in a later section. The GPD of a scalar system is defined by the matrix elements of bi-local scalar field operators [1, 2, 3, 4]:

$$\mathcal{J}^+ \equiv \frac{1}{2} \int \frac{dz^-}{2\pi} e^{ixP^+z^-} \langle P' | \Phi^\dagger(0) \tilde{\partial}^+ \Phi(z) | P \rangle \Big|_{z^+=z^\perp=0} = \mathcal{H}(x, \zeta, t), \quad (1)$$

where x is the conventional Bjorken variable, ζ the so-called skewedness parameter, and $\tilde{\partial} = \bar{\partial} - \partial$. The elastic electromagnetic form factor of a system composed of two scalar particles is given by:

$$J^+ \equiv \langle P' | \Phi^\dagger(0) \tilde{\partial}^+ \Phi(0) | P \rangle = (P + P')^+ F(t). \quad (2)$$

It follows directly from these definitions that integrating the GPD over x gives the form factor,

$$\frac{2}{2-\zeta} \int \mathcal{H}(x, \zeta, t) dx = F(t), \quad (3)$$

where the dependence on the skewedness parameter ζ drops out. This result is an important constraint for any model calculation. The normalization is chosen such that $F(0) = 1$.

Let us now present our notation. Any four vector v^μ will be denoted (v^+, v^\perp, v^-) , where the light cone variables are defined by $v^\pm = (v^0 \pm v^3)/\sqrt{2}$ and the transverse part $v^\perp = (v^1, v^2)$. For the kinematics indicated in Fig. 1, we introduce the ratios

$$x = \frac{p^+}{P^+}, \quad \zeta = -\frac{\Delta^+}{P^+} \quad (4)$$

of plus-components. With these definitions, which differ from other conventional ones [17, 18], both x and ζ are defined on the interval $[0, 1]$.

We are only going to consider elastic processes, so $P^2 = P'^2 = M^2$ and $\Delta^2 = t$. The following relation is true in general:

$$(\Delta^\perp + \zeta P^\perp)^2 = -\zeta^2 M^2 - (1 - \zeta)t, \quad (5)$$

the positivity of which implies an upper bound for the skewedness ζ at a given value of the momentum transfer t : $\zeta \leq (-t)/(2M^2) \left(\sqrt{1 + 4M^2/(-t)} - 1 \right) \leq 1$.

III. SCALAR ELECTRODYNAMICS

Let us start with the simplest model which allows for a completely analytic solution of the Bethe-Salpeter equation: this model describes a bound state of two distinguishable equal-mass scalar particles bound together by a zero-range interaction. For later convenience, we chose only one of the constituent particles to be charged. Our Lagrangian is,

$$\mathcal{L} = [D_\mu \phi]^\dagger [D^\mu \phi] - m^2 \phi^\dagger \phi + \frac{1}{2} \partial_\mu \chi \partial^\mu \chi - \frac{1}{2} m^2 \chi^2 - \frac{g}{2} (\phi^\dagger \phi \chi^2), \quad (6)$$

with $D_\mu = \partial_\mu + ieA_\mu$ so that the electromagnetic charge only couples to the field ϕ . Assuming that the coupling constant g is much larger than the electromagnetic coupling constant e , we have bound states stemming from the last term in Eq. (6). The corresponding Bethe-Salpeter equation is trivially solved in ladder approximation, providing the fully covariant amplitude for the bound state of total mass $M^2 = P^2$:

$$\Phi(P, p) = \frac{C}{(m^2 - p^2) (m^2 - (P - p)^2)}, \quad (7)$$

where p is the four-momentum of one of the two constituents with equal mass m , and C is a normalization constant. The spectrum for the ground state in this model is given by

$$1 = -igI(P), \quad (8)$$

where the integral $I(P)$ is given by Eq. (B2). Note that this integral is actually divergent, so some sort of renormalization would be required in order to calculate the spectrum. The theory defined by Eq. (6) is renormalizable and a renormalization program for bound states can be defined. However, for the evaluation of parton distribution functions in this model, we do not encounter any divergent integrals, we shall therefore ignore any matters of renormalization.

The model defined by the above equations is certainly not realistic enough to furnish a reasonable description of real, physical bound states, like the pion for instance. Its main advantage lies in its simplicity, the fact that one may obtain analytic solutions without approximations that violate physical requirements or symmetries, like Lorentz- or Gauge invariance, sum rules, etc and moreover it has the added advantage that it is defined within a renormalizable quantum field theory. These properties make it a useful playground to perform benchmark calculations, as it was used recently in order to test the viability of certain relativistic quantum mechanics approaches [19, 20].

A. Generalized parton distribution function

Our starting point is to write the Generalized Parton distribution (GPD) as an integral over Bethe-Salpeter amplitudes. To do so we could use Eq. (1) as we shall do in the NJL case. But in an intuitive way, the GPD can be described with the help of Eq. (3), which relates our calculation with the electromagnetic form factor. This procedure arises from the scattering process $\gamma^* + \pi \rightarrow \gamma + \pi$, where the leading “hand-bag” diagram reduces to the triangle diagram of the electromagnetic form factor, since the deep inelastic limit contracts the propagator with infinite momentum (see first diagram in Fig. 1):

$$\begin{aligned} \mathcal{H}(x, \zeta, t) &= -\frac{i}{2} \int \frac{d^4 p}{(2\pi)^4} \delta(p^+ - xP^+) \bar{\Phi}(P, p) (\Delta + 2p)^+ [(P - p)^2 - m^2] \Phi(P + \Delta, p + \Delta) \\ &= \frac{2x - \zeta}{2} \frac{1}{i} \int \frac{d^4 p}{(2\pi)^4} \delta(x - p^+/P^+) \bar{\Phi}(P, p) [(P - p)^2 - m^2] \Phi(P + \Delta, p + \Delta). \end{aligned} \quad (9)$$

Using the Bethe-Salpeter amplitude of Eq. (7), we obtain

$$\mathcal{H}(x, \zeta, t) = \frac{2x - \zeta}{2} \frac{C^2}{i} \int \frac{d^4 p}{(2\pi)^4} \frac{\delta(x - p^+/P^+)}{(p^2 - m^2) [(p + \Delta)^2 - m^2] [(P - p)^2 - m^2]}. \quad (10)$$

Inspecting the pole structure of the integrand for the evaluation of the p^- integral, we note that it vanishes unless $0 \leq x \leq 1$, i.e., the GPDs have the correct support properties. The integral of Eq. (10) may be calculated explicitly. The analytic result for the GPD is then simply

$$\mathcal{H}(x, \zeta, t) = \frac{C^2}{16\pi^2} \frac{2x - \zeta}{2} \tilde{M}(m, x, \zeta, t), \quad 0 \leq x \leq 1, \quad (11)$$

with $\tilde{M}(m, x, \zeta, t)$ given by Eq. (B8). We observe that our result is explicitly covariant, depending only on x , ζ and t . Note that the complete solution is explicitly continuous at $x = \zeta$, however, the derivative at this point is discontinuous. We furthermore encounter a zero at the point $x = \zeta/2$, which is due to the photon vertex, see Eq. (9). The quark distribution function is given by

$$q(x) \equiv \mathcal{H}(x, 0, 0) = \frac{C^2}{16\pi^2} \frac{x(1-x)}{m^2 - x(1-x)M^2}. \quad (12)$$

The normalization integral may be done analytically and determines the normalization constant C .

As it is not a common practice to write GPDs as integrals over Bethe-Salpeter amplitudes, we note that we can write $\mathcal{H}(x, \zeta, t)$ for $x > \zeta$ as the product of light cone wave functions [21], defined by:

$$\Psi(x, p^\perp) \equiv \frac{P^+ x(1-x)}{i\pi} \int dp^- \Phi(P, p) = -\frac{Cx(1-x)}{(p^\perp - xP^\perp)^2 + m^2 - x(1-x)M^2}, \quad (13)$$

which is non-zero only for $0 < x < 1$. Using some kinematic relations, the GPD for $x > \zeta$ may then be written as

$$\mathcal{H}(x, \zeta, t) \Big|_{x>\zeta} = \frac{1}{2} \frac{2x - \zeta}{2} \frac{(1 - \zeta)}{x(1-x)(x - \zeta)} \int \frac{d^2 p^\perp}{(2\pi)^3} \Psi^* \left(\frac{x - \zeta}{1 - \zeta}, p^\perp + \frac{1 - x}{1 - \zeta} \Delta^\perp \right) \Psi(x, p^\perp). \quad (14)$$

On the other hand, for $x < \zeta$, the GPD may not directly be written as the product of light front wave functions like in Eq. (14), even though we are still able to find analytic solutions for the integral of Eq. (10).

In Fig. 2 we give examples of GPDs in this model for different values of the binding energy and momentum transfers. We checked numerically that the sum rule of Eq. (3) is always exactly satisfied. A more stringent test is the so-called polynomiality condition [2, 3, 9], which states that the moments of the GPDs,

$$\int_0^1 dx x^{N-1} \mathcal{H}(x, \zeta, t) \equiv F_N(\zeta, t), \quad (15)$$

give functions $F_N(\zeta, t)$ that are polynomials in ζ of order not higher than N . It is difficult to verify this analytically in the general case, even with the exact solutions that we obtained. Just in the limiting case $M^2 = 0$, the following relation may be shown to hold:

$$F_N(\zeta, 0) = 3 \frac{2N + (N-2) \sum_{i=1}^N \zeta^i}{N(N+1)(N+2)}, \quad (16)$$

i.e., the polynomiality condition is exactly satisfied at zero momentum transfer. Note also that for $N = 1$, Eq. (16) gives the correct normalization of Eq. (3) for any value of ζ . This shows explicitly that the sum rule is indeed independent of ζ in this case.

In the small binding limit, $M^2 \rightarrow 4m^2$, we recover the peaked nature of the GPDs, that was observed in ref. [22], where also an interpretation was given. For small binding energies, the constituents are almost free, so their wave function is highly peaked in momentum space. The two peaks at $x = 1/2$ and $x = (1 + \zeta)/2$ correspond just to the maxima of the corresponding wave function in the overlap formula Eq. (14). In the exact limit $M^2 = 4m^2$, the GPDs reduce to a sum of two δ -functions¹:

$$\mathcal{H}(x, \zeta, t) = \frac{1}{2} \left[\delta \left(x - \frac{1}{2} \right) + \delta \left(x - \frac{\zeta + 1}{2} \right) \right] \frac{2 - \zeta}{2} F(t). \quad (17)$$

In particular, the quark distribution function $q(x) = \mathcal{H}(x, 0, 0)$ becomes simply $q(x) = \delta(x - 1/2)$, which means that the particles are free. On the other hand, in the deep binding limit, $M^2 = 0$, and at zero momentum transfer, $t = 0$, we find the simple form

$$\mathcal{H}(x, \zeta, 0) = 6 \frac{2x - \zeta}{2} \left\{ \frac{x}{\zeta} \theta(\zeta - x) + \frac{1 - x}{1 - \zeta} \theta(x - \zeta) \right\}. \quad (18)$$

¹ Note that the form factor in this limit is equal to zero everywhere except at $t = 0$, where it is 1.

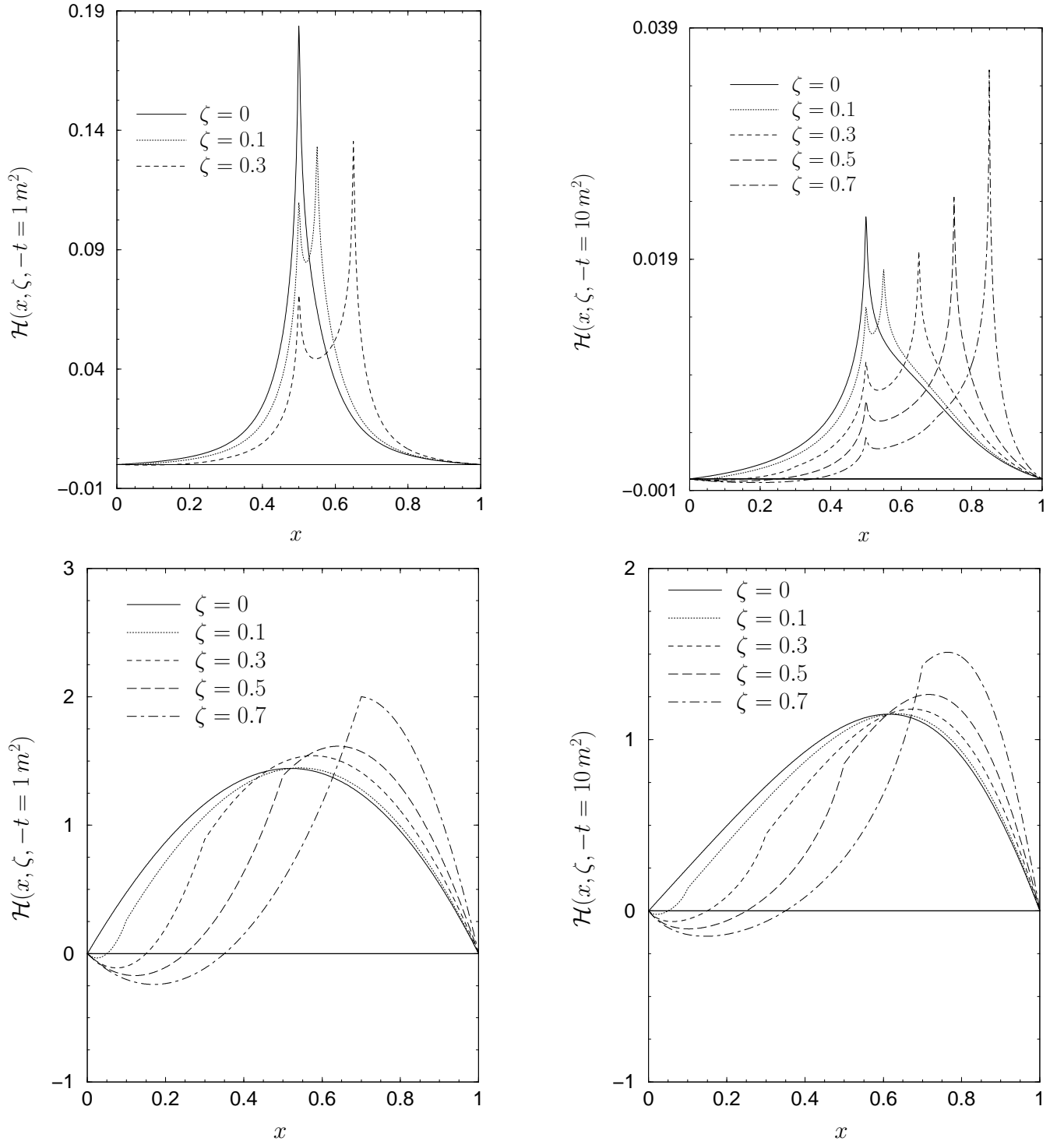


FIG. 2: Generalized parton distributions in the zero-range interaction model for different values of the bound state mass M and momentum transfers t . The top row gives results for $M/m = 2 - (1/137)^2/4$, while on the bottom $M = 0$. The graphs in the left column are for a momentum transfer $-t = 1 m^2$, and on the right, $-t = 10 m^2$. Note that the sum rule of Eq. (3) is exactly satisfied for each graph.

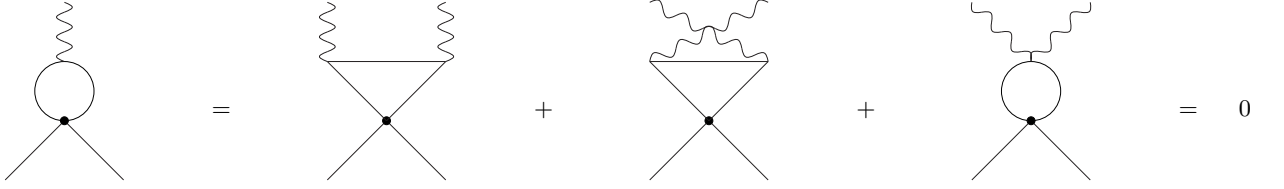


FIG. 3: The second diagram of Fig. 1 contains the loop diagram shown on the left, which corresponds to the expanded set of diagrams on the right, including the seagull term. All of them are divergent, but their sum is not. Moreover when we sum them exactly also there finite parts vanish. The reason behind this cancellation is that the charge is not renormalized to order g .

B. Electromagnetic form factor

Calculating the electromagnetic form factor according to Eq. (2), we find:

$$(P + P')^\mu F(Q^2) = iC^2 \int \frac{d^4 p}{(2\pi)^4} \frac{(\Delta + 2p)^\mu}{(p^2 - m^2) [(p + \Delta)^2 - m^2] [(P - p)^2 - m^2]}, \quad (19)$$

leading to [20],

$$F(Q^2) = \frac{C^2}{16\pi^2} \int_0^1 dz \frac{2}{Q} \frac{1-z}{\sqrt{D}} \log \frac{\sqrt{D} + zQ}{\sqrt{D} - zQ} \equiv \frac{2}{2-\zeta} \int_0^1 dx \mathcal{H}(x, \zeta, t), \quad (20)$$

with $D = 4[m^2 - z(1-z)M^2] + z^2Q^2$. This suggests that one could calculate the GPD by a simple change of the integration variable in the expression for the form factor. The general character of this change of variable would not be clear, however. Naturally, at $Q^2 = 0$ we reproduce the normalization condition.

Taking the parameters $m = 241 \text{ MeV}$ and $M = 139 \text{ MeV}$, we can evaluate the root-mean squared radius of a pion, built of scalar particles, via $\langle r_\pi \rangle^2 = -6 \partial F(Q^2) / \partial Q^2 = (0.47 \text{ fm})^2$, to be compared to the experimental value of $(0.66 \text{ fm})^2$. In the limit of a mass-less bound state, $M = 0$, we obtain the analytic result $\langle r_\pi \rangle^2 = 3/(10m^2) = (0.45 \text{ fm})^2$.

C. Contribution of the second diagram in Fig. 1.

Up to first order in the strong coupling constant g , we have to calculate the second Feynman diagram of Fig. 1. In scalar electrodynamics, the second diagram does not contribute to the electromagnetic form factor. The loop integral is proportional to

$$\int \frac{d^4 q}{(2\pi)^4} \frac{(2q + \Delta)^\mu}{(q^2 - m^2 + i\epsilon)((q + \Delta)^2 - m^2 + i\epsilon)}, \quad (21)$$

which by virtue of Eq. (B4) is zero. However, this diagram could contribute to the GPDs, because here we keep the $+$ component of the integration variable fixed. In a naive way we observe that the bubble present in the diagram will lead to divergent contributions to the GPDs. In order to understand properly the problem let us consider the DVCS on the pion. We note that the bubble corresponds to a triangle in which one of the propagators has been contracted due to the infinite momentum carried by the parton. Divergences appear in the calculation and correspond in practice to terms proportional to $\log(Q^2)$ in the triangle diagram. Considering all contributions to the same order (see Fig. 3), we find that the divergences cancel. But not only the divergent terms cancel, also the finite parts do, therefore the whole contribution, contrary to expectations, vanishes exactly for the GPDs.

It is not difficult to advance a physical argument explaining this cancellation. The diagrams of Fig. 3 can be interpreted as a renormalization of the bare charge present in the seagull term. Due to gauge symmetry this charge must be the square of the charge associated to the one photon vertex, before and after renormalization. But we have seen from Eq. (21) that there is no renormalization (finite or infinite) at order g to the charge. Consequently the sum of diagrams of Fig. 3, or the second diagram of Fig. 1, must vanish.

IV. THE MODEL OF NAMBU AND JONA-LASINIO

The model of the last section can certainly not provide a very realistic description of electromagnetic properties of a pion because of the scalar nature of the constituents involved. We are therefore going to consider a model with spinor particles. An evident choice to investigate is the model of Nambu and Jona-Lasinio (NJL) [15, 23, 24, 25]. This model is the most realistic model for pions built of quarks that is based on a quantum field theory. It gives a good description of the low energy physics of the pion, exhibiting the phenomena of dynamical mass generation and spontaneous breaking of chiral symmetry, which are crucial ingredients for low-energy hadronic physics [15, 16].

We start from the Lagrangian density in the two-flavor version of this model where we add the electromagnetic interaction in the usual way,

$$\mathcal{L} = \bar{\psi}(i\not{D} - \mu_0)\psi + g \left[(\bar{\psi}\psi)^2 - (\bar{\psi}\vec{\tau}\gamma_5\psi)^2 \right], \quad (22)$$

with $D_\mu = \partial_\mu + ieA_\mu$. Again, assuming the contact interaction of the last term to be mainly responsible for the binding, the Bethe-Salpeter equation in ladder approximation to be fulfilled by a bound state in this model is given by (the factor 2 comes from the symmetry of the interaction):

$$S^{-1}(p) \Phi(P, p) S^{-1}(p - P) = ig\vec{\tau}\gamma_5 \int 2\text{Tr} \left\{ \vec{\tau}\gamma_5 \Phi(P, p') \right\} \frac{d^4 p'}{(2\pi)^4}. \quad (23)$$

Here, the symbol Tr refers to traces on spinor, flavor and color indices, and $S(p)$ is the single quark propagator

$$S(p) = \frac{i}{\not{p} - m + i\epsilon} = i \frac{\not{p} + m}{p^2 - m^2 + i\epsilon}, \quad (24)$$

of a quark with constituent mass m , which is generated from the bare mass μ_0 via the gap equation [15, 25]. The quantity $\Phi(P, p)$ is the momentum space image of the Bethe-Salpeter amplitude of a bound state with total four-momentum P , while p is the four-momentum of one of the constituents. The solution of Eq. (23) is rather trivial since the integral on the right hand side is just a constant, so we can write

$$\Phi(P, p) = igCS(p)\vec{\tau}\gamma_5 S(p - P) = -igC \frac{(\not{p} + m)\vec{\tau}\gamma_5(\not{p} - \not{P} + m)}{(p^2 - m^2)[(P - p)^2 - m^2]}, \quad (25)$$

where C is a normalization constant. Reinserting this solution into Eq. (23) and using the definitions Eqs. (B1, B2) for the occurring integrals, gives a self-consistency condition,

$$1 = 4N_c N_f ig [2I_1 - P^2 I(P)], \quad (26)$$

which determines the mass of the ground state as a function of the coupling constant. Note that in the chiral limit, when $P^2 = 0$, Eq. (26) is nothing but the gap equation, providing some evidence for the self-consistency of the procedure.

The NJL model has been investigated quite excessively in different domains of physics with rather impressive success (see refs. [15, 25] for reviews), it is therefore natural to test its predictions for GPDs of the pion. Similar studies have been carried out recently [7, 26, 27, 28, 29] with different models. One drawback of the NJL model is of course its non-renormalizability, which makes it useful only as an effective, low-energy model that, however, may be regarded as a non-linear realization of the QCD Lagrangian. Numerical results therefore usually depend on the regularization scheme employed to deal with the divergent integrals. As thoroughly discussed in refs. [30, 31], a suitable regularization method has to satisfy a certain number of requirements. The method that was found to be most suitable was a Pauli-Villars with two subtractions, this is the one that we shall adopt, as outlined in appendix A.

A. Generalized parton distribution

We are interested in calculating the hand-bag diagrams of Fig. 4 in the Nambu – Jona-Lasinio Model. A general expression for the matrix element of the bi-local fermionic current in the Bethe-Salpeter approach is

$$\begin{aligned} \langle P' | \bar{\Psi}(x')\gamma_\mu \Psi(x) | P \rangle &= \int d^4 x_2 \text{Tr} \left\{ \bar{\Phi}_{P'}(x', x_2)\gamma_\mu [\Phi_P(x, x_2)(i\vec{\not{\partial}}^{(2)} - m_2)] \right\} \\ &\quad + \int d^4 x_1 \text{Tr} \left\{ \bar{\Phi}_{P'}(x_1, x)(i\vec{\not{\partial}}^{(1)} - m_1)\Phi_P(x_1, x')\gamma_\mu \right\}, \end{aligned} \quad (27)$$

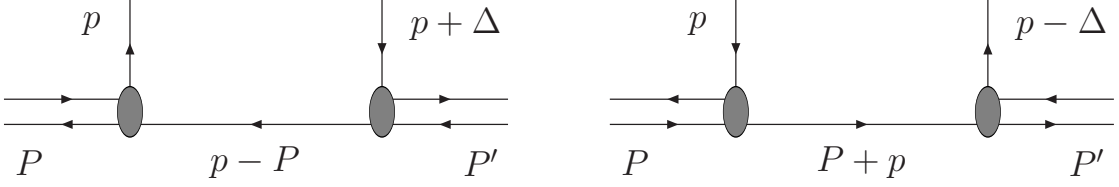


FIG. 4: Hand-Bag diagrams in the Nambu – Jona-Lasinio Model.

where the first (second) term in this expression corresponds to the contribution of the first (second) constituent of the system, and indices 1 and 2 refer to coordinates or operators related to particles 1 and 2 bound in the meson. In terms of momentum variables we have

$$\Phi_P(x_1, x_2) = e^{-iP \cdot X} \int \frac{d^4 k}{(2\pi)^4} e^{-ikr} \Phi(k, P), \quad (28)$$

with the center-of-mass and relative coordinates defined by

$$X = \mu_1 x_1 + \mu_2 x_2, \quad r = x_1 - x_2, \quad \mu_{1,2} = \frac{m_{1,2}}{m_1 + m_2}, \quad (29)$$

and $P = p_1 + p_2$, $k = \mu_2 p_1 - \mu_1 p_2$ the total and relative four-momentum of the system. We shall concentrate on the u -quark parton distribution in a π^+ meson, for which we have to consider the first diagram of Fig. 4, with $p_1 = p$, $p_2 = P - p$. The second diagram of Fig. 4 would correspond to the d -quark parton distribution with $p_1 = -p$, $p_2 = P + p$. Inserting Eq. (28) and taking $m_1 = m_2 = m$, we have for the hand-bag contribution to the GPD:

$$\begin{aligned} \frac{1}{2} \int \frac{dz^-}{2\pi} e^{ixP^+ z^-} \langle P' | \bar{\Psi}(0) \gamma^+ \Psi(z) | P \rangle \Big|_{z^+ = z^- = 0} &= \mathcal{H}(x, \zeta, t) = \\ &= \frac{1}{2} \int \frac{d^4 p}{(2\pi)^4} \delta(x - p^+ / P^+) \text{Tr} \left\{ \bar{\Phi}(p + P' - P, P') \gamma^+ \Phi(p, P) (\not{p} - \not{P} - m) \right\}, \end{aligned} \quad (30)$$

where we have switched back to particle momenta. With the Bethe-Salpeter amplitude of Eq. (25) and its adjoint $\bar{\Phi}(P, p)$, we obtain an expression for the GPD in the Nambu – Jona-Lasinio model that is similar to Eq. (10):

$$\mathcal{H}(x, \zeta, t) = i \frac{4N_c N_f g^2 C^2}{2} \int \frac{d^4 p}{(2\pi)^4} \delta(x - p^+ / P^+) \frac{(x + 1 - \zeta)(p^2 - m^2) + p \cdot \Delta - xP \cdot \Delta - (2x - \zeta)p \cdot P}{(p^2 - m^2)[(p + \Delta)^2 - m^2][(P - p)^2 - m^2]}. \quad (31)$$

The p^- integral in Eq. (31) is evaluated by the usual residue calculus. Due to the pole structure of the integrand we obtain two contributions, the first one in the region $\zeta < x < 1$, corresponding to the quark contribution and the second in the region $0 < x < \zeta$, corresponding to a quark-anti-quark contribution. The second diagram of Fig. 4 will give an anti-quark contribution in the region $\zeta - 1 < x < 0$, and a sea-quark contribution in the region $0 < x < \zeta$, just like the first diagram. In case of a π^+ meson, the first diagram gives the u -quark distribution, while the second one gives the \bar{d} -quark distribution, but due to iso-spin symmetry, both distributions are related by $\mathcal{H}_u(x, \zeta, t) = -\mathcal{H}_{\bar{d}}(\zeta - x, \zeta, t)$. Concentrating only on the u -quark distribution and employing a Pauli-Villars regularization, we get for $1 > x > \zeta$:

$$\begin{aligned} \mathcal{H}(x, \zeta, t) \Big|_{x > \zeta} &= \frac{2N_c N_f g^2 C^2}{16\pi^2} \sum_{j=0}^2 c_j \left\{ -\log \frac{m_j^2}{m^2} - \frac{1}{2} \log \frac{m_j^2 - \bar{x}M^2}{m_j^2} - \frac{1}{2} \log \frac{m_j^2 - \bar{y}M^2}{m_j^2} \right. \\ &\quad \left. + \frac{(2x - \zeta)M^2 + (1 - x)t}{2} \tilde{M}(m_j, x, \zeta, t) \right\}, \end{aligned} \quad (32)$$

with the abbreviations $\bar{x} = x(1 - x)$, $\bar{y} = (1 - x)(x - \zeta)/(1 - \zeta)^2$, while $\tilde{M}(m, x, \zeta, t)$ is given by Eq. (B8) with $m = m_0$. We note that the first three terms in the curly bracket of Eq. (32) give contributions that are independent of the momentum transfer t . The first term, in particular, gives an overall constant, independent of x , ζ and t , which does not vanish for $x = 1$. From Eq. (32) we get the normal distribution function at zero momentum transfer,

$$q(x) = \mathcal{H}(x, 0, 0) = \frac{2N_c N_f g^2 C^2}{16\pi^2} \sum_{j=0}^2 c_j \left\{ -\log \frac{m_j^2}{m^2} - \log \frac{m_j^2 - \bar{x}M^2}{m_j^2} + \frac{m_j^2}{m_j^2 - \bar{x}M^2} \right\}, \quad (33)$$

TABLE I: The moments of the GPDs, as defined by Eq. (15), for the pion in various models. SED and NJL give the analytic results in the chiral limit, $M = 0$, for the scalar model, Eq. (16), and the model of Nambu – Jona-Lasinio, Eq. (36), respectively. $F_N^v = F_N(\zeta = 0, t = 0)$ and $F_N^{nv} = F_N(\zeta = 1, t = 0)$ represent pure valence and pure non-valence contributions, respectively.

Model	$F_2^v [F_2^{nv}]$	$F_3^v [F_3^{nv}]$	$F_4^v [F_4^{nv}]$	$F_5^v [F_5^{nv}]$	$F_6^v [F_6^{nv}]$	$F_7^v [F_7^{nv}]$
ref. [28] ^a	0.503 [0.312]	0.312 [0.217]	0.215 [0.161]	0.16 [0.125]	0.123 [0.101]	0.098 [0.083]
ref. [32]		0.29 [—]				
SED	$\frac{1}{2} [\frac{1}{2}]$	$\frac{3}{10} [\frac{9}{20}]$	$\frac{1}{5} [\frac{2}{5}]$	$\frac{1}{7} [\frac{5}{14}]$	$\frac{3}{28} [\frac{9}{28}]$	$\frac{1}{12} [\frac{7}{24}]$
NJL	$\frac{1}{2} [\frac{1}{3}]$	$\frac{1}{3} [\frac{1}{4}]$	$\frac{1}{4} [\frac{1}{5}]$	$\frac{1}{5} [\frac{1}{6}]$	$\frac{1}{6} [\frac{1}{7}]$	$\frac{1}{7} [\frac{1}{8}]$

^aThe results for F_N^{nv} of this reference have been divided by a factor 2, in order to comply with a different definition of variables.

which determines the normalization condition. Turning our attention to the non-valence region, for $0 < x < \zeta$ we find:

$$\mathcal{H}(x, \zeta, t) \Big|_{x < \zeta} = \frac{2N_c N_f g^2 C^2}{16\pi^2} \sum_{j=0}^2 c_j \left\{ -\log \frac{m_j^2}{m^2} - \frac{1}{2} \log \frac{m_j^2 - \bar{x}M^2}{m_j^2} - \frac{2x/\zeta - 1}{2} \log \frac{m_j^2 - \bar{y}t}{m_j^2} + \frac{(2x - \zeta)M^2 + (1 - x)t}{2} \tilde{M}(m_j, x, \zeta, t) \right\}, \quad (34)$$

where now $\bar{y} = x(\zeta - x)/\zeta^2$. A few properties of the final result may immediately be recognized. First, the total GPD is again continuous at $x = \zeta$, even though the derivative at this point is not. Second, as noted above, $\mathcal{H}(1, \zeta, t) \neq 0$, but from Eq. (34) we see that $\mathcal{H}(0, \zeta, t) = 0$ for $\zeta \neq 0$. Third, we note that at $x = 1$, the GPD becomes independent of t and ζ , it only depends on the bound state mass M via the normalization constant $g^2 C^2$. In particular, in the chiral limit, when $M^2 = 0$, the value of $\mathcal{F}(x, \zeta, t)$ at $x = 1$ is simply given by

$$\mathcal{H}(1, \zeta, t) = 1. \quad (35)$$

In spite of these peculiarities, we find again that Eq. (3) is always exactly satisfied, as we checked numerically. In addition, the polynomiality condition takes a very simple form in the chiral limit. When $M^2 = 0$, the following relation may be shown to hold:

$$F_N(\zeta, 0) = \frac{1}{N} \left(1 - \frac{\zeta^N}{N+1} \right), \quad (36)$$

i.e., at zero momentum transfer, the polynomiality condition is fulfilled. Again, for $N = 1$, Eq. (36) reproduces Eq. (3) in the case $t = 0$. In Table I we give a comparison of moments of GPDs in the scalar model, the NJL model and results of other works. We see a rather nice agreement of the NJL results with those of ref. [28], especially for low moments, while for larger N , our results tend to be somewhat larger. The most striking difference appears for the non-valence contributions in the scalar model, which are about a factor of 2 larger than in the NJL model (note that for $t = 0$, the skewedness parameter ζ is actually confined to be zero, see the remark after Eq. (5), but like in ref. [28], we use our analytical formulas, Eqs. (16,36), to continue the results to $\zeta = 1$). Another interesting feature evidenced by the results in this table is the apparent identity

$$F_N^{nv} = F_{N+1}^v, \quad (37)$$

which is analytically fulfilled in the NJL model, see Eq. (36), but also seems to hold for the numerical results of ref. [28]. Only in the scalar model this relation does not hold due to the larger values of the non-valence contributions mentioned above.

Finally we note that in the chiral limit, $M^2 = 0$ and at zero momentum transfer, $t = 0$, we reproduce the analytic results of ref. [7], namely:

$$\mathcal{H}(x, \zeta, 0) = \frac{x}{\zeta} \theta(\zeta - x) + \theta(x - \zeta), \quad (38)$$

so in particular, $\mathcal{H}(x, 1, 0) = x$ and $\mathcal{H}(x, 0, 0) = 1$. This form may be compared with the corresponding result in the scalar model, see Eq. (18). Eq. (38) also implies that in the chiral limit we get a quark distribution function that is equal to unity. This coincides with the results obtained in refs. [31, 33, 34].

In Fig. 5 we give some examples of GPDs in the NJL model. They illustrate two distinct behaviors characterized by the strength of the binding, i.e., the weak and strong binding limits. For zero binding, there is no spontaneous symmetry breaking, thus no pion and the constituents are free. For weak binding, we expect therefore a very similar behavior of the GPDs to the one discussed in scalar electrodynamics. This similarity can be seen by comparing the corresponding graphs of Figs. 2 and 5. In the weak binding limit we note again the appearance of two peaks at $x = 1/2$ and $x = (1 + \zeta)/2$, which go over into δ -functions in the exact limit $M^2 = 4m^2$, just as in the scalar case, see Eq. (17).

As soon as there is binding, chiral symmetry is spontaneously broken, and the GPDs differ more and more from the free ones as we approach the $M = 0$ limit with massive constituent quarks. The most striking feature evidenced by these figures is the non-vanishing of the distribution functions at the boundary, $x = 1$, and (for $\zeta = 0$) $x = 0$. As mentioned above, the value at $x = 1$ is independent of Q^2 and ζ , it only depends on the binding energy, varying from zero, in the free case, to unity in the deep binding limit of zero pion mass. In the NJL model, this effect is associated with the breaking of chiral symmetry, as we shall discuss in more detail later on. The value for $x = 0$, $\zeta = 0$, does depend on Q^2 (decreasing like $1/Q^2$ for large Q^2), but for fixed Q^2 , it depends on the binding energy in the same way as the value at $x = 1$, vanishing again only in the zero-binding limit. Furthermore, the distribution functions become relatively more concentrated around $x = 1$ for large Q^2 , which is just a consequence of the constant value of the distribution function at $x = 1$.

Note also that for large $Q^2 = -t$, the distribution functions become negative in the central region. This can not be seen from the graphs displayed in Fig. 5, but it is a consequence of the relative sign between the terms of the coefficient of the last logarithm in Eq. (32).

B. Electromagnetic form factor

In order to understand better the above results, we may want to calculate the electromagnetic form factor in the NJL model which is given by the x -integrated parton distribution, see Eq. (3). This has been done already in several works [15, 35, 36], but we want to investigate the relation with the present results. Calculating again the current in impulse approximation, (the second diagram of Fig. 1 vanishes again as in the scalar case, for the form factor and for the GPDs), we find:

$$(P + P')^\mu F(Q^2) = 4iN_c N_f g^2 C^2 \int \frac{d^4 p}{(2\pi)^4} \frac{(p^\mu + P^\mu + \Delta^\mu)(p^2 - m^2) + p \cdot \Delta P^\mu - P \cdot \Delta p^\mu - (2p^\mu + \Delta^\mu) p \cdot P}{(p^2 - m^2) [(p + \Delta)^2 - m^2] [(P - p)^2 - m^2]}. \quad (39)$$

Rewriting the denominator under the integral and using some relations of appendix B, we arrive at

$$F(Q^2) = iN_c N_f g^2 C^2 \frac{(Q^2/2 + M^2)I(\Delta) + M^2 I(P) - M^4 M(\Delta, -P)}{Q^2/4 + M^2}. \quad (40)$$

We checked numerically (by applying the same Pauli-Villars regularization method) that this form factor is exactly reproduced by integrating our result for the GPD over x . This means that the non-vanishing distribution functions (at $x = 1$) are implicitly present in the result of Eq. (40). Note that in the chiral limit, $M^2 = 0$, we simply have

$$F(Q^2) = 2iN_c N_f g^2 C^2 I(\Delta) = 1 - R(Q^2)/I(0), \quad (41)$$

where for small Q^2 , $R(Q^2)$ is given by

$$R(Q^2) = \frac{i}{16\pi^2} \frac{Q^2}{6m^2}, \quad (42)$$

so together with the relation $f_\pi^2 = -12im^2 I(0)$, we can evaluate the root-mean squared radius of the pion in this model via $\langle r_\pi \rangle^2 = -6 \partial F(Q^2)/\partial Q^2 = 3f_\pi^{-2}/(4\pi^2)$, which is the same as in ref. [15]. With $f_\pi = 93$ MeV, we find the numerical value of $\langle r_\pi \rangle^2 = (0.585 \text{ fm})^2$, to be compared to the experimental value of $(0.66 \text{ fm})^2$. Note, however, that Eq. (42) is valid only in the limit when the cut-off goes to infinity, for the finite cut-off as specified in appendix A, the root mean squared radius gets multiplied by a factor ~ 0.89 .

V. DISCUSSION

The results obtained in the scalar electrodynamics model show a perfect realization of all wishful ingredients. The calculation is exact, finite and satisfies all the desired properties, i.e., the GPDs have the correct support and vanish at

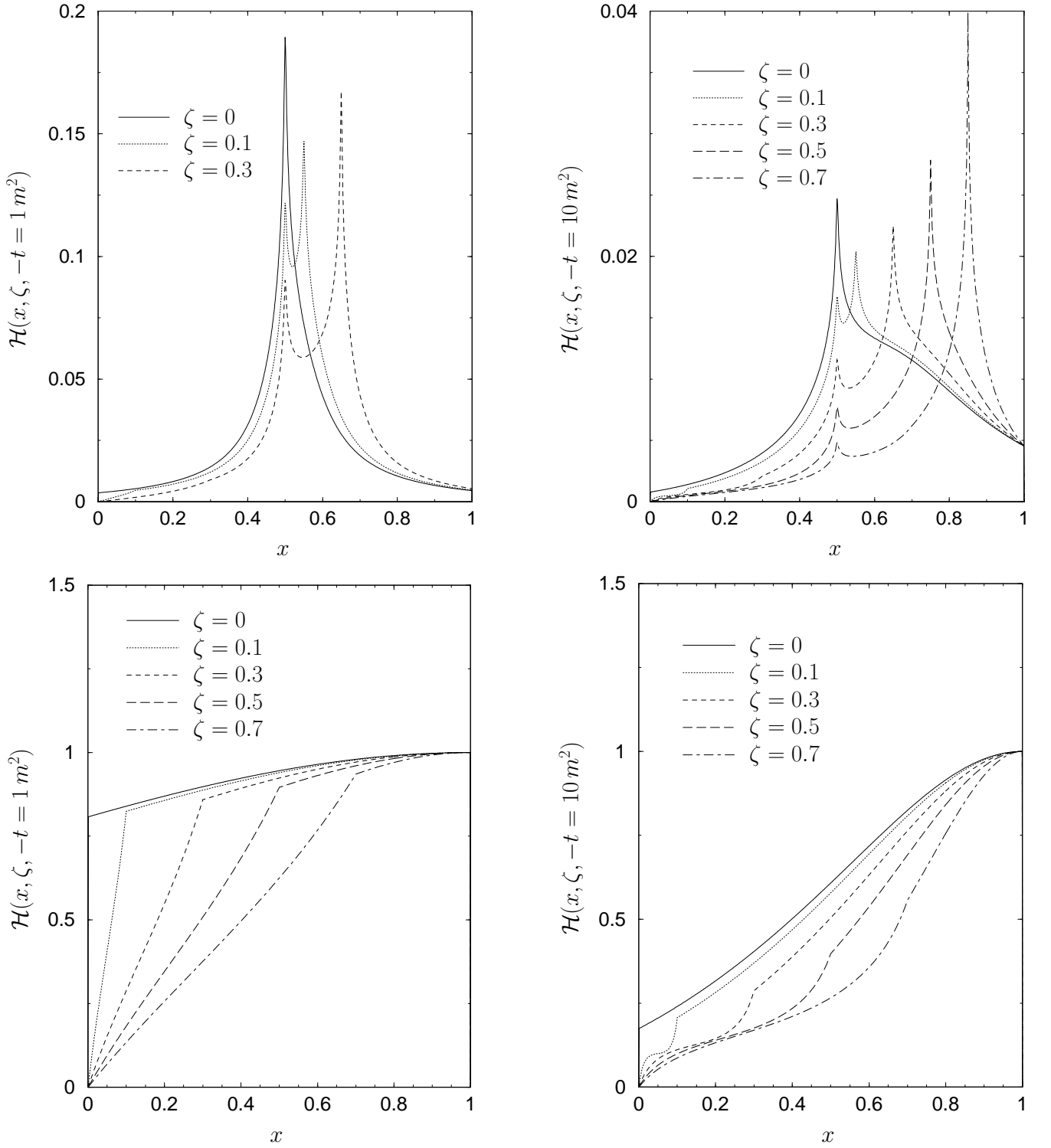


FIG. 5: Generalized parton distributions in the Nambu – Jona-Lasinio model for different values of the bound state mass M and momentum transfers t . The top row gives results for $M/m = 2 - (1/137)^2/4$, while on the bottom $M = 0$ MeV. The graphs in the left column are for a momentum transfer $-t = 1 m^2$, and on the right, $-t = 10 m^2$. Note that the sum rule of Eq. (3) is exactly satisfied for each graph.

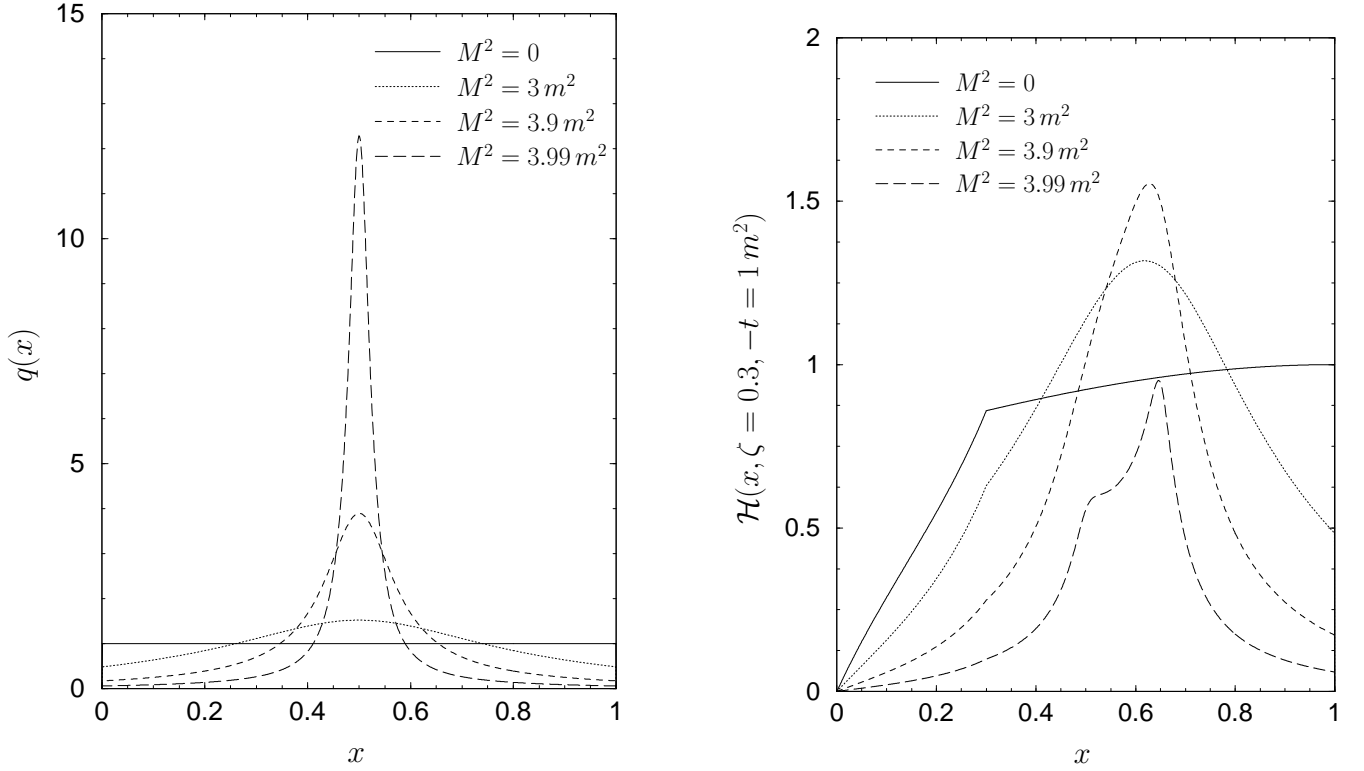


FIG. 6: Generalized parton distribution functions in the Nambu – Jona-Lasinio model as functions of x for different bound state masses M . On the left figure we have the quark distribution function $q(x) = \mathcal{H}(x, 0, 0)$, on the right we have $\mathcal{H}(x, \zeta = 0.3, -t = 1 m^2)$. The constituent mass is kept fixed at $m = 241$ MeV.

the boundary regions, while the sum rule and the polynomiality condition are exactly verified. From the physical point of view, the GPDs show a realization in terms of quasi-free constituents in the weak binding limit. As the binding increases one is confronted with the dynamics as derivable from a non trivial momentum distribution determined by the corresponding Bethe-Salpeter amplitude, a feature also appearing in other model calculations [14]. The physical effect associated with t and ζ is naturally represented in the GPDs. The variable t tends to push the constituent distribution towards higher values of x , which corresponds to an input of momentum transfer into the system, while the variable ζ incorporates the description of virtual pairs. Unfortunately this model is not very realistic for the pion (perhaps it might be better fit for a description of the nucleon) and our results represent only qualitative features of how the dynamics might influence the distributions.

An equivalent model was considered in refs. [22, 37], but the emphasis was put on the light-front quantization method. Consequently, the results were defined only for $x > \zeta$, while the region $x < \zeta$ was explored by an analytic continuation of the vertex function. However, sum rules like the one appearing in Eq. (3) are explicitly violated in this approach.

For the NJL model the calculation requires regularization. The latter certainly influences the results, as has been discussed in ref. [30], where the Pauli-Villars method was compared to the one of Brodsky-Lepage with different results. The Pauli-Villars method is compatible with all the symmetry requirements [33], which is the reason for our choice. A caveat that should be emphasized is that the model does not only contain the dynamics expressed in the Lagrangian, but also the one derived from the regularization procedure.

The NJL calculation retains some nice properties, in particular it preserves the sum rule and the polynomiality condition. Physically it is also very appealing since we can distinguish features associated with the weak and strong coupling regimes. In Fig. 6 we show on the left hand side the variation of the quark distribution function with the binding energy. As the binding energy increases we change softly from a delta type behavior, at zero binding, to a constant behavior in the strong binding regime. This figure also illustrates nicely the phase transition associated with the spontaneous breaking of chiral symmetry. Suppose we keep the mass of the bound state fixed at $M^2 = 0$ and consider the variation of $q(x)$ with the constituent mass m . It is clear that we will always have $q(x) = 1$ for any value of m , except when $m = 0$, where the distribution function changes discontinuously to $q(x) = \delta(x - 1/2)$. The

effects of t and ζ described for scalar electrodynamics persist, as can be seen in the graph on the right hand side of this figure, i.e., t pushes the distribution to higher values of x and ζ introduces virtual pairs into the description of the system.

The problem we face is the non-vanishing of the GPDs at the boundary, i.e., $\mathcal{H}(x, \zeta, t) \neq 0$ for $x = 1$ and (if $\zeta = 0$) $x = 0$. For the structure function $q(x) = \mathcal{H}(x, 0, 0)$, this feature was already noted in refs. [31, 33, 34] and it is obviously present in an implicit way in the results of electromagnetic form factor calculations [15, 35, 36]. It showed up already in several model calculations [7, 38, 39, 40, 41]. Various ad hoc solutions have been implemented to deal with this problem. In refs. [7, 38], a momentum dependent constituent quark mass (or equivalently, a constituent quark form factor) was introduced to force the distribution functions to be zero at the end points, while in ref. [39] the problem was resolved by applying the QCD evolution equations [42]. Curiously, we did not find a discussion of this peculiarity, with respect to its physical interpretation, in any of these references.

To elucidate the matter, one might investigate the mass dependence of the GPDs at a given point x . In our calculation we get for $x = 1$ the general expression

$$\mathcal{H}(x = 1, \zeta, t) = \frac{F_0}{F_0 - 1 + \left(\sqrt{\frac{4m^2}{M^2} - 1} + \frac{1}{\sqrt{\frac{4m^2}{M^2} - 1}} \right) \arctan \left(\frac{1}{\sqrt{\frac{4m^2}{M^2} - 1}} \right) + \dots}, \quad (43)$$

where $F_0 = 16i\pi^2 I(0)$, with $I(p)$ given by Eq. (B6), is a regularization constant, and the dots denote terms of higher order in M^2/Λ^2 , where Λ is the cut-off parameter in the Pauli-Villars regularization, see Appendix A. This equation illustrates the dependence on the bound state mass, and also the regularization scheme dependence is apparent. It is clear from Eq. (43) that $\mathcal{H}(x = 1, \zeta, t)$ vanishes for zero binding ($M^2 = 4m^2$) while it is non-vanishing for $M^2 < 4m^2$. As soon as the interaction binds the quarks into a pion, $M^2 < 4m^2$ and at the same time, chiral symmetry is spontaneously broken. Therefore, our previous observation, that the non-zero value at $x = 1$ is related to chiral symmetry breaking, is justified. Moreover in the NJL model we recover the result that in the chiral limit, $M^2 = 0$, $q(x)$ is independent of x and equal to unity. It must be recalled that this feature also arises in the 't Hooft model [43], where one finds $q(x) = \text{const.}$ for zero-mass pions.

It has to be stressed that the feature of a non-vanishing distribution function at the end-points in our model has nothing to do with what is usually called the support problem. The latter is characterized by a non-vanishing distribution function outside the physical region, i.e. $\mathcal{H}(x, \zeta, t) \neq 0$ for $x < \zeta - 1$ or $x > 1$, while in our calculations, the GPDs explicitly vanish there. It is therefore really a discontinuity that we encounter at the physical boundary.

The physical interpretation of this feature is not completely clear at present. Let us however conjecture a solution to it based on a analysis of known results. The usual idea that the parton distributions must vanish on the boundary is based in the study of free parton models. If one of the partons carries all the $+$ component of the momentum, i.e. $x = 1$, the other has $p^+ = 0$ and thus p^- goes to infinity. Since this p^- enters the propagator, the obvious conclusion is that the parton distribution must vanish at this boundary. But this simple description is broken when the particles are off-shell, like those in a bound system. Our result is therefore not unnatural. Moreover, the fact that the distributions do not vanish at $x = 0$ for $\zeta = 0$ is just a consequence of the non-vanishing at $x = 1$ and does not seem to introduce any new conceptual problem.

One could suspect that this feature may originate as an artifact of the regularization in the NJL model, but this suspicion should be immediately dropped since it also occurs in the 't Hooft model, which is exact. Therefore we are inclined to think that there is a deeper physical reason for it, and the reason behind it lies in the off-shellness of the bound state quarks and chiral symmetry, as described above.

Let us be more precise. In the chiral limit both models produce a structure function $q(x)$ which is equal to 1 for any value of x . The similitude in behavior is striking and is the reason behind our suspicion. Nevertheless, when chiral symmetry is explicitly broken, the model of 't Hooft leads to a structure function which vanishes at the endpoints, $q(x = 0) = q(x = 1) = 0$, while the NJL does not. This difference is not surprising since the two models contain very different physics, i.e. the 't Hooft model is confining, its interaction is not a point interaction and it is a 1+1 dimensional model. We do not believe that the number of dimensions plays a fundamental role in this phenomenon, but we have no way to determine which of the other two properties is responsible for the different behavior shown at the boundaries.

It has been recently shown [44] that the interpretation of quark structure functions as probability distributions is not necessarily correct because final state interactions between the scattered and the spectator particle affect the structure functions profoundly. This statement strongly supports our line of thought. A strict mathematical proof seems however not easy to find.

VI. CONCLUSION

In this work, we presented a detailed calculation of generalized parton distribution functions using a covariant Bethe-Salpeter approach both in scalar electrodynamics and in the Nambu – Jona-Lasinio model. No assumptions have gone into the determination of the Bethe Salpeter amplitudes or any other ingredient of the calculation. The only approximations employed are the ladder approximation for the determination of the Bethe - Salpeter bound state amplitude (which is, of course, still a fully covariant object in this case), and in the determination of the current matrix elements, we have restricted ourselves to the impulse approximation. In addition, we have shown that the lowest order correction to the impulse approximation vanishes exactly. As a result of this procedure, no important features required by general physical considerations, like symmetry properties, sum rules, etc., have been violated and we recover them in our numerical results. For the scalar model, the calculation evidences all desirable features, we recover results obtained in similar studies, extend them to other kinematical regions and find sum rules which were not possible in the other treatments. In the case of the NJL model, we found the GPDs for the massive case, and discovered that they do not vanish at the boundary of the kinematic region, i.e., at $x = 0$ and $x = 1$, a feature which seems to be associated with spontaneous chiral symmetry breaking and the off-shellness of the constituent quarks.

Before finishing we must recall that our calculation is valid at the hadronic scale, i.e., at a low momentum renormalization point. Evolution to higher momenta is necessary to describe deep inelastic scattering data. It will be interesting to see how the described features of the NJL model will change under evolution. However the fact that the distributions do not vanish at the boundary imply the appearance of strong singularities which render the process non trivial.

Acknowledgments

This work was supported by the European Commission IHP program under contract HPRN-CT-2000-00130, MCYT (Spain) under contracts BFM2001-3563-C02-01 and BMF2001-0262, and Generalitat Valenciana under contract GV01-216. One of us (V.V.) would like to thank the Physics Department of Seoul National University, and Prof. Dong-Pil Min in particular, for the hospitality extended to him during the last stages of this work.

APPENDIX A: REGULARIZATION

We shall use the Pauli-Villars regularization in order to render the occurring integrals finite. This means that for integrals like the ones defined by Eqs. (B1-B3), we make the replacement

$$\int \frac{d^4 p}{(2\pi)^4} f(p; m^2) \longrightarrow \int \frac{d^4 p}{(2\pi)^4} \sum_{j=0}^2 c_j f(p; m_j^2), \quad (\text{A1})$$

with $m_j^2 = m^2 + j\Lambda^2$, $c_0 = -c_1/2 = c_2 = 1$. Following ref. [15] we determine the regularization parameters Λ and m by calculating the pion decay constant and the quark condensate (in the chiral limit) via

$$f_\pi^2 = -\frac{3m^2}{4\pi^2} \sum_{j=0}^2 c_j \log(m_j^2/m^2), \quad \langle \bar{u}u \rangle = -\frac{3m}{4\pi^2} \sum_{j=0}^2 c_j m_j^2 \log(m_j^2/m^2). \quad (\text{A2})$$

With the conventional values $\langle \bar{u}u \rangle = -(250 \text{ MeV})^3$ and $f_\pi = 93 \text{ MeV}$, we get $m = 241 \text{ MeV}$ and $\Lambda = 859 \text{ MeV}$.

APPENDIX B: ELEMENTARY INTEGRALS

$$I_1 \equiv \int \frac{d^4 k}{(2\pi)^4} \frac{1}{k^2 - m^2 + i\epsilon}, \quad (\text{B1})$$

$$I(p) \equiv \int \frac{d^4 k}{(2\pi)^4} \frac{1}{(k^2 - m^2 + i\epsilon)((k+p)^2 - m^2 + i\epsilon)}, \quad (\text{B2})$$

$$M(p_1, p_2) \equiv \int \frac{d^4 k}{(2\pi)^4} \frac{1}{(k^2 - m^2 + i\epsilon)(k_1^2 - m^2 + i\epsilon)(k_2^2 - m^2 + i\epsilon)}, \quad (\text{B3})$$

with $k_i = k + p_i$. From these definitions the following relation may be deduced:

$$\int \frac{d^4 k}{(2\pi)^4} \frac{k^\mu}{(k^2 - m^2 + i\epsilon)((k+p)^2 - m^2 + i\epsilon)} = -\frac{1}{2}p^\mu I(p). \quad (\text{B4})$$

With the Pauli-Villars regularization of Eq. (A1) we have the following simple expressions:

$$I_1 = -\frac{i}{16\pi^2} \sum_{j=0}^2 c_j m_j^2 \log(m_j^2/m^2), \quad (\text{B5})$$

$$I(p) = -\frac{i}{16\pi^2} \sum_{j=0}^2 c_j \left\{ \log(m_j^2/m^2) + \sqrt{\frac{p^2 - 4m_j^2}{p^2}} \log \frac{1 - \sqrt{\frac{p^2 - 4m_j^2}{p^2}}}{1 + \sqrt{\frac{p^2 - 4m_j^2}{p^2}}} \right\}. \quad (\text{B6})$$

To obtain the results of Eqs. (11,32,34), we used the following formulas:

$$\tilde{I}(P) \equiv -16i\pi^2 \int \frac{d^4 k}{(2\pi)^4} \frac{\delta(x - k^+/P^+)}{(k^2 - m^2 + i\epsilon)((k-P)^2 - m^2 + i\epsilon)} = \begin{cases} \sum_{j=0}^2 c_j \log \frac{m_j^2 - \bar{x}P^2}{m^2}, & 0 < x < 1, \\ 0 & \text{otherwise.} \end{cases} \quad (\text{B7})$$

$$\begin{aligned} \tilde{M}(m, x, \zeta, t) &\equiv -16i\pi^2 \int \frac{d^4 k}{(2\pi)^4} \frac{\delta(x - k^+/P^+)}{(k^2 - m^2 + i\epsilon)((k+\Delta)^2 - m^2 + i\epsilon)((P-k)^2 - m^2 + i\epsilon)} = \\ &= \begin{cases} \frac{1}{\sqrt{D}} \log \frac{[2(1-\zeta)(\zeta y - x) - \zeta]M^2 - (1-x)t + 2m^2/y + \sqrt{D}}{[2(1-\zeta)(\zeta y - x) - \zeta]M^2 - (1-x)t + 2m^2/y - \sqrt{D}}, & 0 < x < 1, \\ 0 & \text{otherwise.} \end{cases} \end{aligned} \quad (\text{B8})$$

In the last integral, $D = \zeta^2 M^2 (M^2 - 4m^2) + (1-x)^2 t^2 + 2(1-x)(2x-\zeta)M^2 t - 4m^2(1-\zeta)t$, $\zeta = -\Delta^+/P^+$, $M^2 = P^2$, $t = \Delta^2$ and

$$y = \begin{cases} x/\zeta, & 0 < x < \zeta, \\ (1-x)/(1-\zeta), & \zeta < x < 1. \end{cases} \quad (\text{B9})$$

-
- [1] D. Müller, D. Robaschik, B. Geyer, F. M. Dittes, and J. Horejsi, Fortschr. Phys. **42**, 101 (1994), hep-ph/9812448.
 - [2] X.-D. Ji, Phys. Rev. **D55**, 7114 (1997), hep-ph/9609381.
 - [3] A. V. Radyushkin, Phys. Rev. **D56**, 5524 (1997), hep-ph/9704207.
 - [4] X.-D. Ji, J. Phys. **G24**, 1181 (1998), hep-ph/9807358.
 - [5] M. Diehl, T. Feldmann, R. Jakob, and P. Kroll, Eur. Phys. J. **C8**, 409 (1999), hep-ph/9811253.
 - [6] M. Diehl, T. Feldmann, R. Jakob, and P. Kroll, Nucl. Phys. **B596**, 33 (2001), hep-ph/0009255.
 - [7] M. V. Polyakov and C. Weiss, Phys. Rev. **D60**, 114017 (1999), hep-ph/9902451.
 - [8] M. Diehl, T. Feldmann, P. Kroll, and C. Vogt, Phys. Rev. **D61**, 074029 (2000), hep-ph/9912364.
 - [9] X.-D. Ji, W. Melnitchouk, and X. Song, Phys. Rev. **D56**, 5511 (1997), hep-ph/9702379.
 - [10] I. V. Anikin, D. Binosi, R. Medrano, S. Noguera, and V. Vento, Eur. Phys. J. **A14**, 95 (2002), hep-ph/0109139.
 - [11] V. Y. Petrov et al., Phys. Rev. **D57**, 4325 (1998), hep-ph/9710270.
 - [12] M. Penttinen, M. V. Polyakov, and K. Goeke, Phys. Rev. **D62**, 014024 (2000), hep-ph/9909489.
 - [13] S. Scopetta and V. Vento (2002), hep-ph/0207218.
 - [14] S. Scopetta and V. Vento (2002), hep-ph/0201265.
 - [15] S. P. Klevansky, Rev. Mod. Phys. **64**, 649 (1992).
 - [16] J. Bijnens, Phys. Rept. **265**, 369 (1996), hep-ph/9502335.
 - [17] K. J. Golec-Biernat and A. D. Martin, Phys. Rev. **D59**, 014029 (1999), hep-ph/9807497.

- [18] P. A. M. Guichon and M. Vanderhaeghen, *Prog. Part. Nucl. Phys.* **41**, 125 (1998), hep-ph/9806305.
- [19] B. Desplanques, L. Theußl, and S. Noguera, *Phys. Rev.* **C65**, 038202 (2002), nucl-th/0107029.
- [20] A. Amghar, B. Desplanques, and L. Theußl (2002), nucl-th/0202046.
- [21] S. J. Brodsky, M. Diehl, and D. S. Hwang, *Nucl. Phys.* **B596**, 99 (2001), hep-ph/0009254.
- [22] B. C. Tiburzi and G. A. Miller, *Phys. Rev.* **C64**, 065204 (2001), hep-ph/0104198.
- [23] Y. Nambu and G. Jona-Lasinio, *Phys. Rev.* **122**, 345 (1961).
- [24] Y. Nambu and G. Jona-Lasinio, *Phys. Rev.* **124**, 246 (1961).
- [25] U. Vogl and W. Weise, *Prog. Part. Nucl. Phys.* **27**, 195 (1991).
- [26] I. V. Anikin, A. E. Dorokhov, A. E. Maksimov, L. Tomio, and V. Vento, *Nucl. Phys.* **A678**, 175 (2000).
- [27] C. Vogt, *Phys. Rev.* **D64**, 057501 (2001), hep-ph/0101059.
- [28] H.-M. Choi, C.-R. Ji, and L. S. Kisslinger, *Phys. Rev.* **D64**, 093006 (2001), hep-ph/0104117.
- [29] L. S. Kisslinger, H.-M. Choi, and C.-R. Ji, *Phys. Rev.* **D63**, 113005 (2001), hep-ph/0101053.
- [30] R. M. Davidson and E. Ruiz Arriola (2001), hep-ph/0110291.
- [31] R. M. Davidson and E. Ruiz Arriola, *Phys. Lett.* **B348**, 163 (1995).
- [32] A. V. Belitsky, *Phys. Lett.* **B386**, 359 (1996), hep-ph/9604329.
- [33] H. Weigel, E. Ruiz Arriola, and L. P. Gamberg, *Nucl. Phys.* **B560**, 383 (1999), hep-ph/9905329.
- [34] T. Shigetani, K. Suzuki, and H. Toki, *Phys. Lett.* **B308**, 383 (1993), hep-ph/9402286.
- [35] V. Bernard and U. G. Meissner, *Phys. Rev. Lett.* **61**, 2296 (1988).
- [36] H. J. Schulze, *J. Phys.* **G20**, 531 (1994).
- [37] B. C. Tiburzi and G. A. Miller, *Phys. Rev.* **D65**, 074009 (2002), hep-ph/0109174.
- [38] M. Praszalowicz and A. Rostworowski (2002), hep-ph/0205177.
- [39] E. R. Arriola and W. Broniowski (2002), hep-ph/0207266.
- [40] A. E. Dorokhov and L. Tomio, *Phys. Rev.* **D62**, 014016 (2000).
- [41] I. V. Anikin, A. E. Dorokhov, and L. Tomio, *Phys. Lett.* **B475**, 361 (2000), hep-ph/9909368.
- [42] D. Müller, *Phys. Rev.* **D51**, 3855 (1995), hep-ph/9411338.
- [43] G. 't Hooft, *Nucl. Phys.* **B75**, 461 (1974).
- [44] S. J. Brodsky, P. Hoyer, N. Marchal, S. Peigné, and F. Sannino, *Phys. Rev.* **D65**, 114025 (2002), hep-ph/0104291.